Journal of Advanced Joining Processes 3 (2021) 100041

Contents lists available at ScienceDirect

Journal of Advanced Joining Processes

journal homepage: www.elsevier.com/locate/jajp

Microstructural deformation in the clinching process

Sia A. Nourani, Dirk J. Pons*, Abbas Tamadon, Digby Symons

University of Canterbury, New Zealand

ARTICLE INFO

Keywords:
Electron backscatter diffraction (EBSD)
Clinching
Shear band
Microstructure
Misorientation

ABSTRACT

Need – There is a need to better understand the shear and plastic deformation that arises during clinch joint formation. Since microstructural texture preserves a history of deformation, grain structure has the potential to reveal the role of the operational parameters. Objective – This study elucidates the grain morphology of clinched joints using electron backscattering diffraction (EBSD) microscopy. Results – The main characteristics of grain morphology are equiaxed grains in the base material, with markedly elongated grain morphology and smaller grains in the necked region. Interpretation – The morphology is attributed to extensive plastic deformation causing the mechanochemical effect of dynamic recrystallization whereby localised recrystallization occurs along with transformation of grain morphology, followed by subsequent solutionizing and precipitation. Originality - An explanation is provided for the microstructural transformations during the clinching process.

Introduction

Clinching is a rapid metal deformation joining process for sheet materials. Though well-established, it is an ongoing area of research (Peng et al., 2020; Lei et al., 2019; Lin et al., 2020). The principle of operation is that a punch tool locally deforms the two sheets plastically to create an interlocking button (Tenorio et al., 2019; Song et al., 2019; Bayraktar and Cerkez, 2020). The result is similar to spot welding, but without the need for thermal processes.

The plastic deformation process in clinching is imperfectly understood. This is important because of the risk of diminished strength of the bond (Lei et al., 2019; Tekkaya et al., 2020). In particular there is a need to better understand the shear that arises during joint formation (He, 2017; Gibmeier et al., 2002). This is difficult to analyse because of the extreme plastic deformation.

There is an opportunity for a material science contribution here. In general, microstructural texture preserves a history of deformation. Grain structure has the potential to reveal the role of the operational parameters, as has been shown in related deformation situations (Sun et al., 2019; Tamadon et al., 2020). The method most suited to reveal grain structure is electron backscattering diffraction (EBSD) microscopy. This is capable of elucidating crystallographic misorientation, grain boundary network, grain size, and morphology. The technique has been widely used to study shear and strain behaviours, e.g. (Zhu et al., 2016; Monajati et al., 2020; Mironov et al., 2020). However, EBSD has not previously been shown in the literature for clinched joints.

The objective of the present study was to elucidate the grain morphology of clinched joints using EBSD.

Experimental approach

Commercial cold rolled steel sheet (JIS G3141-SPCC SD) was used with thicknesses of 1.2 mm and 0.8 mm for upper and lower sheets respectively. Sheets of the same thickness were cut from one coil to ensure equivalent mechanical properties. Chemical and mechanical properties of this material are summarised in Table 1 and Table 2, respectively.

A servo-hydraulic testing machine (MTS® 810 Material Testing System) was used to apply the force and measure the displacement of the punch. Total movement of the punch was 2.8 mm and the processing time approximately 1 s.

Joints were cross-sectioned with a low-speed saw (ISOMET ®). The main geometric parameters of the joint were measured using an optical microscope: bottom thickness, interlock, and neck thickness, see Fig. 2.

The joint sample was separated into the upper and lower sheets, as the focus of the present study was the upper sheet which undergoes the more severe deformation. Specimens were mounted in resin and polished using colloidal silica to 0.02 μm (Buehler ® Beta 2 dual platen grinder-polisher machine equipped with Vector power head).

The microstructural-crystallographic characterization of the samples was performed via EBSD using an HKL Nordlys® III EBSD detector (Oxford Instruments plc, Abingdon, UK) with phase analysis using

* Corresponding author.
E-mail addresses: sia.nourani@pg.canterbury.ac.nz (S.A. Nourani), dirk.pons@canterbury.ac.nz (D.J. Pons), abbas.tamadon@pg.canterbury.ac.nz (A. Tamadon).

https://doi.org/10.1016/j.jajp.2021.100041
Received 3 December 2020; Received in revised form 30 December 2020; Accepted 31 December 2020

Table 1
Typical chemical composition of JIS G3141-SPCC SD.

C (%)	Mn (%)	P (%)	S (%)	Si (%)
6	21	19	18	TR

TR composition: Si (TR) < 0.01%, Mo/Nb/Ti (TR) < 0.001%, B (TR) <0.0001%.

Table 2
Typical mechanical properties of JIS G3141-SPCC SD.

Longitudinal Tensile properties	Specification
0.2% Proof Stress MPa	190
Tensile Strength, MPa	340
% Elongation on gauge length (GL) = 50	42%
HV Hardness	95

Clinched specimens of 6 mm diameter were made by a TOX® clinching die set consisting of a punch (TOX part # 10.180.), a round fixed die (TOX part # 10.25.) and an elastic blank holder. Fig. 1 shows the setup.

an energy-dispersive X-ray spectrometer (EDS) detector (Oxford Instruments plc, Abingdon, UK). Fig. 2 depicts the approximate regions of electron microscopy analysis. Optical micrographs were subsequently obtained after etching with 2% Nital solution, see Fig. 4.

Results

EBSD results

The inverse pole figure (IPF) analysis assigns colour to grains based on the crystal orientation and selected viewing direction. Results show a progressive change in grain structure from base material to the neck, see Fig. 3. The main characteristics of grain morphology are as follows.

For the *base material* (regions 1, 2), the primary cold-rolled grain structure is evident, with an average grain size of 50 μm. Note the different magnifications in the figure. The IPF colour map for the base metal shows a random distribution of the grain orientation for the recrystallized grain structure of the rolled plate. These equiaxed grains contrast with the elongated grain morphology and smaller grains that begin to be apparent in the *pre-necking* region 3 and become highly characteristic in the *necked* regions 4 to 5. The morphology shows distortion in the direction of induced shear, i.e. shear bands are evident.

The *stretched corner*, region 6, shows elongated grains, which is consistent with the expected stretching occurring in this region. The morphology in this region is not as severely distorted, and the grains are larger, than in regions 4–5. The *basal plate*, regions 7–8, show grain

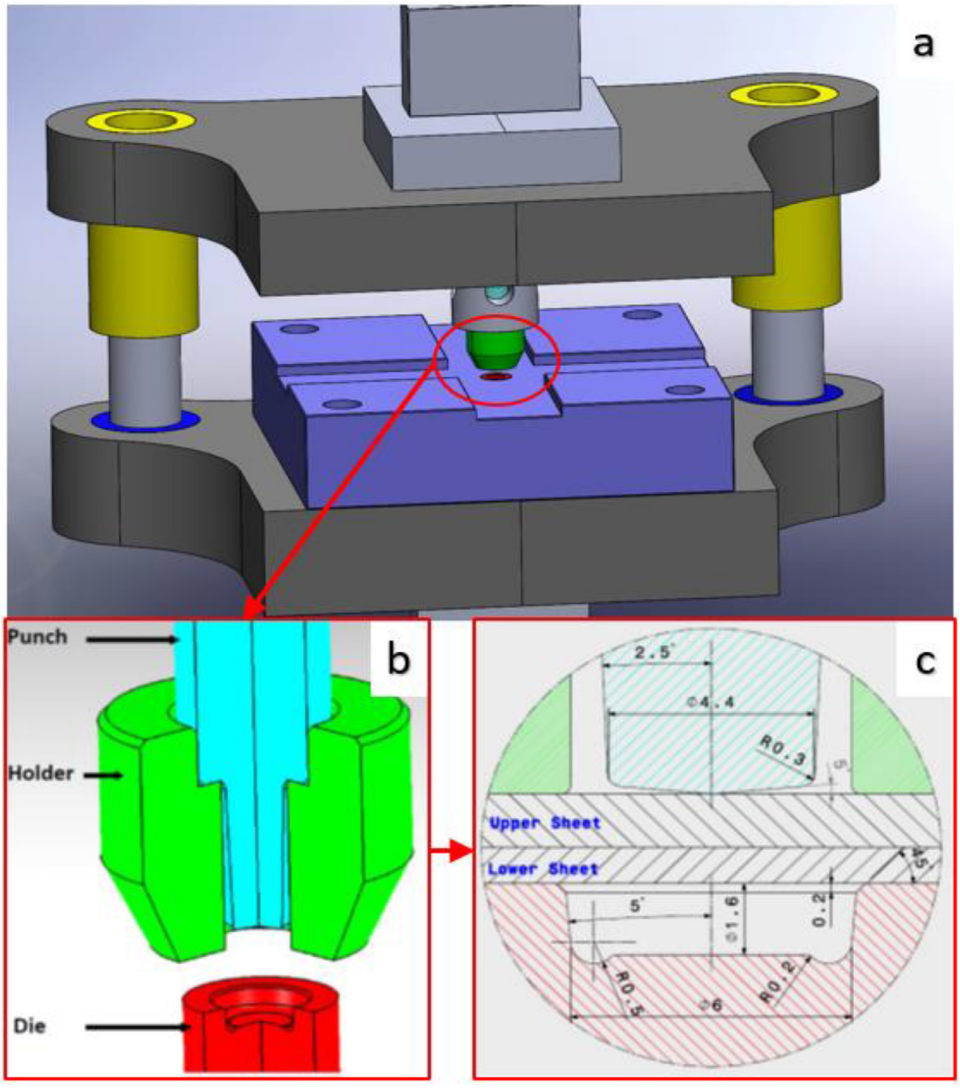

Fig. 1. Clinch tooling (a) Set up of die- set in cross head of testing machine, (b) Detail of punch and die: the punch slides in the holder, and locally presses the two sheets (not shown) into the die.

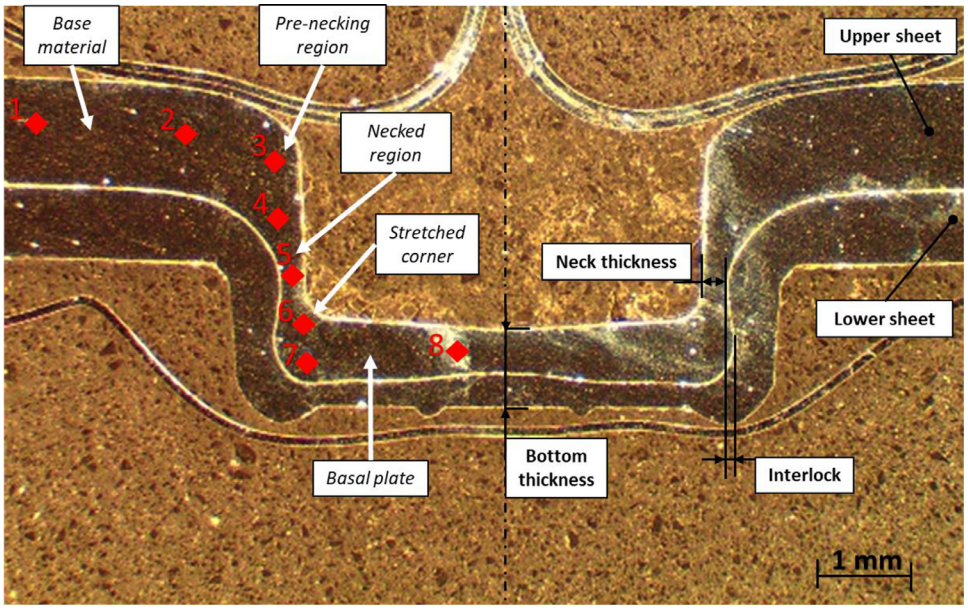

Fig. 2. Cross section of clinched joint and approximate regions of EBSD detection results (regions 1&2: base metal; region 3: prenecking; region 4&5: necking area; region 6: stretched corner; region 7&8: basal plate).

Table 3
EDS results of the phase analysis for different regions of the clinched sample.

Phase Name	Phase Fraction (%)	
	Base-Metal	Clinched-Region
Iron FCC	0.02	0.02
Cementite 2	2.90	0.50
Iron BCC (old)	59.90	70.91
Zero Solutions	37.19	28.57

morphology that are similar to the base material. This suggests these areas are not exposed to the shear in the clinching process. This is consistent with the deep drawing process, where these regions are called dead zones because they do not experience stretching or shear.

Phase transforations

The results of the EDS for both base metal and clinched region are listed in Table 3. The progress of the clinching causes a decrease in phase fraction cementite content, from 2.90% in the base metal to 0.50% for the elongated grains forming the shear band layers. This is along with a decrease in the amount of solutionizing compounds from 37.19% to 28.57%. Subsequently, the BCC iron was increased from 59.90% to 70.91% for the matrix phase of the texture.

This is in agreement with the mechanochemical effect where the unstable phases of the texture can be transformed by dissolving within the crystalline lattice of the BCC iron matrix. It appears that the shearing drives this dissolving process. It is likely this also generates vacancies within the BCC crystal lattice, hence forming the wrinkled-layer pattern of the shear bands (regions 4&5). These shear bands thus represent the direction of the preferential pathway of the atoms where they migrate within the crystal lattice.

Discussion and interpretation of findings

The metallurgical transformations in the clinching process can be anticipated from considerations of general principles of dynamic recrystallization (DRX). In the BCC lattice of the SPCC steel microstructure, the cold-working plastic deformation is expected to cause the formation of sub-grain boundaries, i.e. low-angle grain boundaries (LAGBs). At ambient temperatures, these dislocations form inside the grain as their ability to migrate to the grain boundaries (high-angle grain boundaries) is curtailed by the cool conditions. These subsequently form new grains, hence also smaller grains. The current EBSD results certainly show the change in grain size and orientation, but the sub grain boundaries are less visible than might be expected. In contrast high shear conditions in aluminium friction stir welding readily show sub grain boundaries (Tamadon et al., 2019). Possibly in the present case the ductility of the material (including lack of internal precipitates) causes dislocation not to be arrested within the grain but to rapidly split the grain or propagate to the boundaries.

Another possible DRX transformation is the formation of precipitates at the main grain boundaries where the driving force of the precipitation is higher than other regions of the crystal lattice. There is potential evidence of this in the EBSD maps, where spots are evident at grain boundaries (see for example region 4). These show undetected phases or compounds.

We propose that both processes occurred in the case under examination: the extensive plastic deformation causes the mechanochemical effect of dynamic recrystallization whereby localised recrystallization occurs along with transformation of grain morphology, and subsequent solutionizing and precipitation. This process is summarized in Fig. 4.

This is a similar interpretation made in the literature for other plastic deformation conditions (Sakai et al., 2014). According to the literature (Carneiro and Simões, 2020), this mechanochemical process within the microtexture is related to the transitional state of the grain boundary network under the plastic deformation and subsequent release of the induced strain.

The present results are also consistent with literature for punching where it has been shown that the BCC crystalline structure of SPCC steel demonstrates an alteration from the rolled grain morphology to the elongated grains (Lins).

Conclusions

The originality of this work is to provide an explanation of the microstructural transformations during the clinching process. Our interpretation is that the formation of the elongated grains under shear loading is caused by dynamic recrystallization within the plasticized texture.

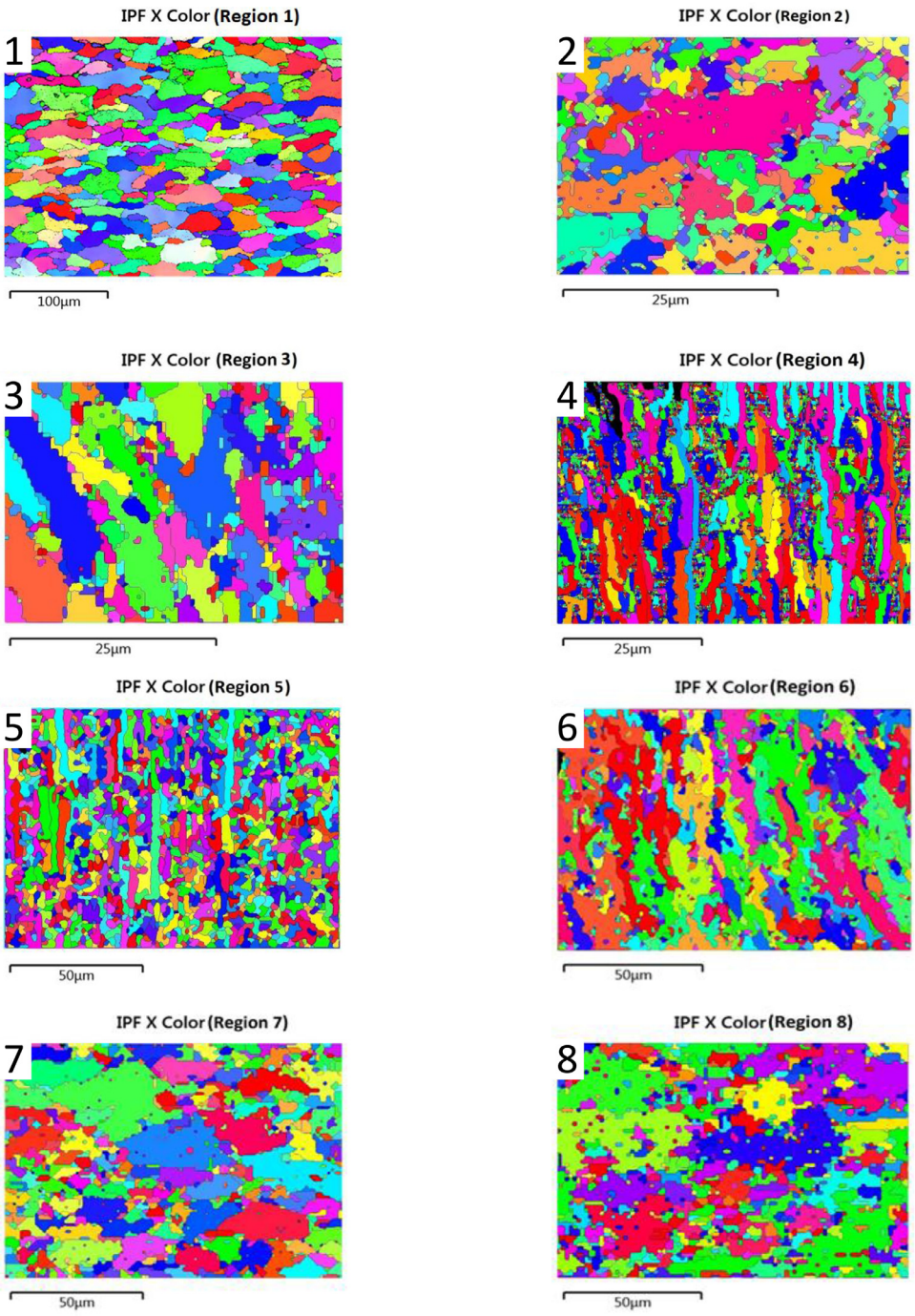

Fig. 3. EBSD analysis IPF map for different locations of the clinched texture, from the base metal to the necking region of the clinched joint. Note the images have a variety of scales.

The shear banding is thus formed by stabilisation of the microstructure in elongated grain morphology.

Contribution statement

Conceptualization, S.N. and D.P.; methodology, S.N. and D.P.; software, S.N. and D.P.; validation, S.N. and D.P.; formal analysis, S.N., A.T. and D.P.; investigation, S.N. and D.P.; resources, D.P.; data curation, S.N. and D.P.; writing—original draft preparation, S.N., A.T. and D.P.; writing—review and editing, S.N., A.T., D.P. and D.S.; visualization, S.N., A.T. and D.P.; supervision, D.P. and D.S.; project administration, D.P.; funding acquisition, D.P. All authors have read and agreed to the published version of the manuscript.

Funding

This research received no external funding.

Declaration of Competing Interest

The authors declare no conflict of interests.

Acknowledgements

Thanks are extended to Shaun Mucalo for assistance with electron microscopy.

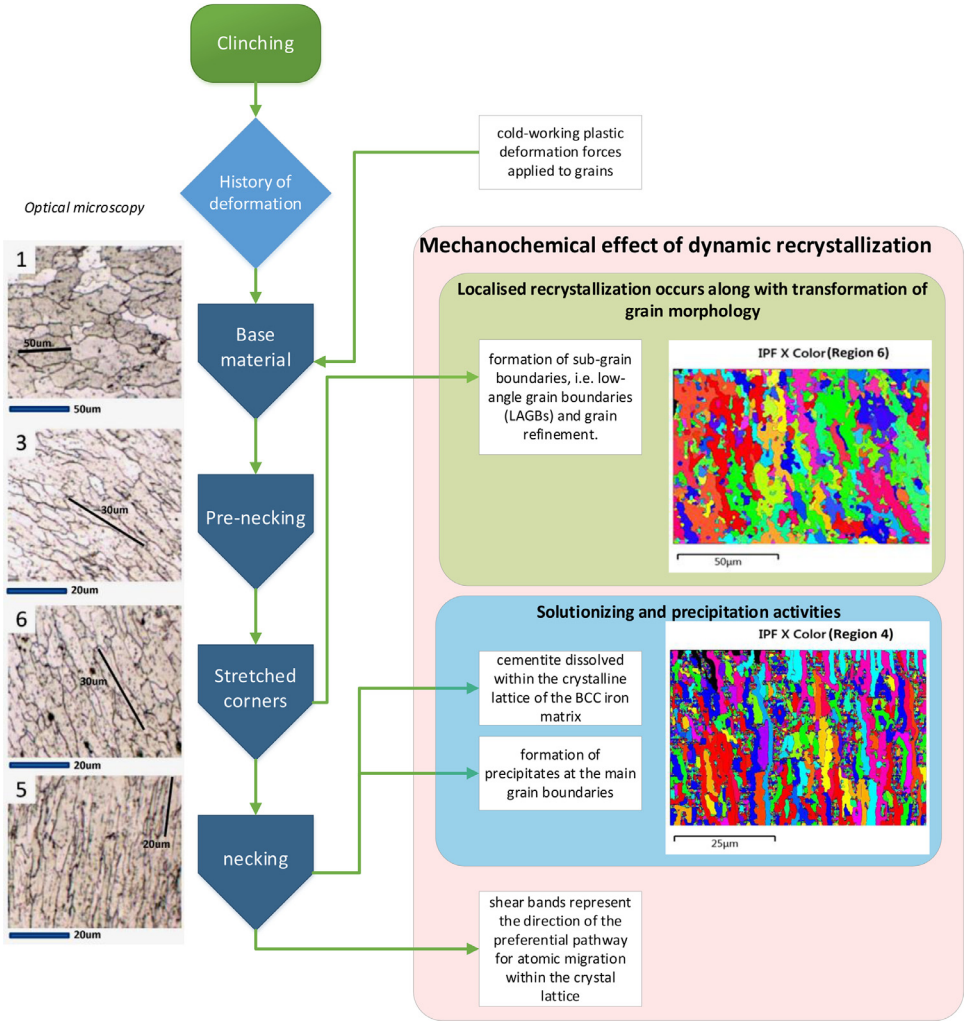

Fig. 4. Explanation of Mechanochemical effect of dynamic recrystallization in the clinching process.

References

Bayraktar, M., Cerkez, V., 2020. Experimental and numerical investigation of clinched joint and implementation of the results to design of a tumble dryer. J. Brazil. Soc. Mech. Sci. Eng. 42, 1–12.

Carneiro, Í., Simões, S., 2020. Recent advances in EBSD characterization of metals. Metals (Basel) 10, 1097.

Gibmeier, J., Rode, N., Peng, R.L., Odén, M., Scholtes, B., 2002. Residual stress in clinched joints of metals. Appl. Phys. A 74, s1440–s1442. doi:10.1007/s003390201431.

He, X., 2017. Clinching for sheet materials. Sci. Technol. Adv. Mater. 18, 381–405. doi:10.1080/14686996.2017.1320930.

Lei, L.; He, X.; Yu, T.; Xing, B. Failure modes of mechanical clinching in metal sheet materials. Thin-Walled Struct. 2019, 144, 106281, doi:10.1016/j.tws.2019.106281.

Lin, P.-.C., Fang, J.-.C., Lin, J.-.W., Tran, X.V., Ching, Y.-.C., 2020. Preheated (Heat-Assisted) Clinching Process for Al/CFRP Cross-Tension Specimens. Materials (Basel) 13, 4170.

Lins, J.; Sandim, H.R.Z.; Vecchio, K.; Raabe, D. An EBSD investigation on deformation-induced shear bands in Ti-bearing IF-steel under controlled shock-loading conditions. In Proceedings of Materials Science Forum; pp. 393-398.

Mironov, S., Sato, Y.S., Kokawa, H., Hirano, S., Pilchak, A.L., Semiatin, S.L., 2020. Microstructural characterization of friction-stir processed Ti-6Al-4V. Metals (Basel) 10, 976.

Monajati, H., Zoghlami, M., Tongne, A., Jahazi, M., 2020. Assessing microstructure-local mechanical properties in friction stir welded 6082-T6 aluminum alloy. Metals (Basel) 10, 1244.

Peng, H., Chen, C., Zhang, H., Ran, X., 2020. Recent development of improved clinching process. Int. J. Adv. Manuf. Technol. 1–31.

Sakai, T.; Belyakov, A.; Kaibyshev, R.; Miura, H.; Jonas, J.J. Dynamic and post-dynamic recrystallization under hot, cold and severe plastic deformation conditions. Progr. Mater. Sci. 2014, 60, 130–207, doi:10.1016/j.pmatsci.2013.09.002.

Song, Y., Yang, L., Zhu, G., Hua, L., Liu, R., 2019. Numerical and experimental study on failure behavior of steel-aluminium mechanical clinched joints under multiple test conditions. Int. J. Lightweight Mater. Manuf. 2, 72–79. doi:10.1016/j.ijlmm.2018.12.005.

Sun, Y., Fujii, H., Sato, Y., Morisada, Y., 2019. Friction stir spot welding of SPCC low carbon steel plates at extremely low welding temperature. J. Mater. Sci. Technol. 35, 733–741. doi:10.1016/j.jmst.2018.11.011.

Tamadon, A., Pons, D.J., Clucas, D., Sued, K., 2019. Texture evolution in AA6082-T6 BFSW welds: optical microscopy and ebsd characterisation. Materials (Basel) 12, 3215. doi:10.3390/ma12193215.

Tamadon, A., Pons, D.J., Clucas, D., 2020. Flow-based anatomy of bobbin friction-stirred weld; AA6082-T6 aluminium plate and analogue plasticine model. Appl. Mech. 1, 3–19. doi:10.3390/applmech1010002.

Tenorio, M.B., Lajarin, S.F., Gipiela, M.L., Marcondes, P.V.P., 2019. The influence of tool geometry and process parameters on joined sheets by clinching. J. Brazil. Soc. Mech. Sci. Eng. 41, 67. doi:10.1007/s40430-018-1539-0.

Tekkaya, A., Bouchard, P.-.O., Bruschi, S., Tasan, C., 2020. Damage in metal forming. CIRP Ann..

Zhu, C., Harrington, T., Livescu, V., Gray III, G.T., Vecchio, K.S, 2016. Determination of geometrically necessary dislocations in large shear strain localization in aluminum. Acta Mater. 118, 383–394. doi:10.1016/j.actamat.2016.07.051.